109941
Copy 2

AEDC-TN-56-1
(AD-84917)

[redacted]

DOCUMENT NO. 109941
This is copy number ____
of 162, which consists of
27 pages, series A.

DECLASSIFIED / UNCLASSIFIED

THE EXTENT AND DECAY OF PRESSURE DISTURBANCES CREATED BY THE HOLES IN PERFORATED WALLS AT TRANSONIC SPEEDS

(TITLE UNCLASSIFIED)

By

H. E. Gardenier; PWT, ARO, Inc.

April 1956

CLASSIFICATION CANCELLED (CHANGED TO Unclassified)
BY AUTHORITY OF AEDC Declassification Notice No. 2 February 19, 1959
BY W. S. Brothers March 9, 1959
Name and Position of Individual Date

ARNOLD ENGINEERING DEVELOPMENT CENTER

AIR RESEARCH AND DEVELOPMENT COMMAND

US AF

DECLASSIFIED / UNCLASSIFIED

[redacted]

AEDC-TN-56-1
(AD-84917)

THE EXTENT AND DECAY OF PRESSURE DISTURBANCES CREATED BY THE HOLES IN PERFORATED WALLS AT TRANSONIC SPEEDS

By

H. E. Gardenier; PWT, ARO, Inc.

April 1956

Contract No. AF 40(600)-620

CONTENTS

ILLUSTRATIONS

SUMMARY

Experimental investigations were made to determine the extent and decay of the pressure disturbances created by the holes in a perforated-wall transonic test section when the flow is parallel to or at a small inclination to the wall. Conventional perforations with holes at a right angle to the wall were tested with several sizes of holes. A single wall with hole axes inclined 60° was also investigated. For the Mach number range of these tests, from 1.0 to 1.2, disturbances on the order of ± 0.01 in Mach number were shown to exist near the wall. These disturbances decayed to a level of ± 0.002 in Mach number within a distance of 25 hole diameters from the wall.

NOMENCLATURE

M	Local Mach number
ΔM	Mach number variation (from mean M)
θ_w	Wall angle, min
Y	Distance from wall, in.
d	Hole diameter, in.
p_s	Local static pressure, psf
p_o	Settling-chamber pressure, psf
δ^*	Boundary-layer displacement thickness, in.

INTRODUCTION

During investigations of transonic test section characteristics in the Transonic Model Tunnel of the Propulsion Wind Tunnel facility at Arnold Engineering Development Center, it became evident that certain performance characteristics were related to the size of the holes in the perforated walls. A wide range of hole sizes and wall thicknesses was tested to determine their pressure-drop characteristics and general performance. Results of this work are reported in Refs. 1 and 2.

It was concluded that the size of the individual holes should be large, in comparison to the boundary-layer displacement thickness, in order to produce stable tunnel operating conditions at a minimum auxiliary-weight flow. However, it is evident that large holes produce their own disturbance fields of expansion and compression waves. Unless these disturbances mix and die out before reaching the tunnel centerline, the test model will be affected.

This investigation was conducted to determine at what distance from the test section wall the pressure distribution becomes essentially uniform for conditions of flow parallel to the walls or at a small angle to the wall. The condition of large inclination, as would be experienced locally in the region of a model, will be the subject of a future investigation.

EQUIPMENT AND PROCEDURE

The tests reported herein were conducted in the 12-in. x 12-in. Transonic Model Tunnel. This is a continuous-flow, open-circuit tunnel operating with an approximately constant stagnation pressure of 2900 psf. Reynolds number for these tests was approximately 5.2 million per foot. A complete description of this facility is given in Ref. 3.

Perforated walls used in these tests were as follows:

Hole Dia., In.	Plate Thickness, In.	Open Area, %	Hole Angle, deg
1/4	1/16	22	0
1/2	1/16	22	0
1	1/16	22	0
1/4	1/4	6	60

Figure 1 is a diagram of the walls tested. The test wall was mounted on one side of the test section. The other three test section walls were 22-percent open with 0.0625-in. diameter perforations. Disturbances from these fine grid walls did not extend beyond 1.5 in. from the walls, and therefore should not have affected the data.

It will be noted from the above table that three of the four wall samples were conventional, that is, the holes were drilled perpendicular to the wall surface. In the case of the fourth sample, the holes were drilled at an inclination of 60^{o} into the flow. The resulting hole shape on the wall surface is actually an ellipse with a major axis of 1/2 in. and a minor axis of 1/4 in. However, for consistency, the hole diameter of this wall is termed 1/4 in.

By means of a traversing static-pressure probe, variations in static pressure were determined at distances from the walls of 1.0 in. to 9.0 in. Pressure readings were recorded every 0.10 in. in the flow direction. The region surveyed was in the downstream portion of the test section where the flow was parallel to the wall, well beyond the flow establishment region. From these readings, it was possible to determine the axial Mach number variations at several distances from the wall. This system produced an accuracy of ± 0.001 in p_s/p_o. The traversing static-pressure probe used is shown in Fig. 2.

It is possible in the Transonic Model Tunnel to change the angle of two of the test section walls. For this test, the wall angle was used to vary the boundary-layer displacement thickness over the perforated wall and to produce flow at a small angle to the walls with greater disturbances at the holes. Parallel test section walls ($\theta_w = 0^{o}$) produced a displacement thickness, δ^*, of approximately 0.09 in. at the survey region. Converging the test section walls one-half a degree ($\theta_w = -30'$) thinned the displacement thickness to 0.06 in.

RESULTS

The local static pressure, p_s, was divided by the stagnation pressure, p_o, and plotted against position in the tunnel. From these curves, average maximum and average minimum values of p_s/p_o were determined, and the corresponding variation in Mach numbers, ΔM, was computed.

CONVENTIONAL PERFORATIONS

A typical pressure distribution at several distances from the wall is shown in Fig. 3. This particular plot is for the 1/2-in. diameter holes at $M = 1.2$ with the walls converged - 30 minutes. The pressure distribution close to the wall indicates the existence of periodic waves which correlate with the hole pattern. As the survey station is moved farther from the wall, the waves become less distinct, and the maximums and minimums decrease. At a distance of seven inches from the wall, the waves have essentially disappeared and the pressure is approaching uniformity. Figure 4 shows the pressure distribution obtained at Mach number 1.00. These data show that no strong disturbances are present at this Mach number.

A large quantity of such data was obtained for several hole sizes. These data were reduced and are presented in summary form as Mach number variation, ΔM, vs distance from the wall/hole diameter, Y/d. Figure 5 shows the results at Mach number 1.20. It appears from this figure--and also from Figs. 6, 7, 10, 11, and 12 -- that the data for all hole sizes correlate reasonably well into a single curve when this form of presentation is used. Thus the nondimensional distance from the wall, Y/d, may be used to describe the disturbance level for any size hole.

Although there is some scatter of the data points in Fig. 5, it is evident for the parallel-wall case that disturbances greater than 0.01 in Mach number exist close to the wall. These irregularities decrease rapidly as the distance from the wall increases. At approximately 25 hole diameters from the wall, the Mach number variation has decreased to approximately 0.002.

At the converged wall setting ($\theta_w = -30'$) with the thinner boundary layer, the disturbances near the wall are somewhat larger; however, the fluctuations also die out rapidly. In this case a similar low level of variations was also reached at a distance of approximately 25 hole diameters from the wall.

At Mach number 1.10, as shown in Fig. 6, the disturbances near the wall are generally less than 0.01 in Mach number for both boundary-layer conditions. At a distance of approximately 25 hole diameters from the wall, the maximum variations were again 0.002 in Mach number. In the case of Mach number 1.00, the results are presented in Fig. 7; lower Mach numbers produce similar results.

HOLE AXES INCLINED

Certain advantageous results are obtained if the axes of perforations are inclined into the stream (Ref. 4). The same tests as described above were conducted with a 6-percent open-area wall with axes of the holes inclined 60°. A typical pressure distribution, at several distances from the wall, is shown in Fig. 8. This particular plot is for the converged-wall case at Mach number 1.20. These results are similar to those obtained with the conventional perforations in that the wave pattern generated by the holes diminishes in strength and regularity as the distance from the wall increases. Figure 9 shows the pressure distribution obtained at Mach number 1.00.

Reducing the data to the Y/d vs ΔM form, as before, yields the results presented in Figs. 10, 11, and 12. The two curves on these plots result from making $\underline{d}$ equal the minor and major axes of the elliptical hole shape. These results correlate more nearly with the results obtained with conventional perforations if the major axis is considered to be effective hole diameter. That is, the minimum level of variations is reached at a distance from the wall of not more than 25 times the major axis of the ellipse.

Although disturbances near the wall are expected to be greater with a thin boundary layer, as in the case of the conventional perforations, the data obtained with the hole axes inclined are not conclusive in this respect. Hence, only one curve is faired through all the data points in Figs. 10, 11, 12.

CONCLUSIONS

A series of experimental investigations was conducted to determine the decay of pressure disturbances created by the holes in a perforated-wall test section, when the flow was parallel to the walls or at a small inclination angle. For wall configurations tested in the Mach number range from 1.0 to 1.2, the following conclusions were drawn:

1. Systematic expansions and compressions are generated by the holes in a perforated-wall test section. Near the wall these systems cause Mach number variations of ±0.01 or greater for parallel walls.

2. The disturbance systems diminish in intensity with increasing distance from the wall.

3. In the case of conventional perforations, the disturbance level was reduced to ±0.002 in Mach number within a distance of approximately 25 hole diameters from the wall.

4. In the case of hole axes inclined, the disturbance level was reduced to ±0.002 in Mach number within a distance of approximately 25 times the major axis of the elliptical hole opening.

REFERENCES

1. Chew, William L. "Wind Tunnel Investigation of Transonic Test Sections--Phase II: Comparison of Results of Tests on Five Perforated-Wall Test Sections in Conjunction with a Sonic Nozzle." AEDC-TR-54-52, March 1955. (~~Confidential~~)

2. Chew, William L. "Experimental and Theoretical Studies on Three-Dimensional Wave Reflection in Transonic Test Sections--Part III: Characteristics of Perforated Test Section Walls with Differential Resistance to Cross-Flow." AEDC-TN-55-44, March 1956. (~~Confidential~~)

3. Gardenier, H. E. "Description of the Transonic Wind Tunnel--Arnold Engineering Development Center." AEDC-TR-54-70, May 1955.

4. Gray, J. D. and Gardenier, H. E. "Experimental and Theoretical Studies on Three-Dimensional Wave Reflection in Transonic Test Sections--Part I: Wind-Tunnel Tests on Wall Interference of Axisymmetric Bodies at Transonic Mach Numbers." AEDC-TN-55-42, March 1956. (~~Confidential~~)

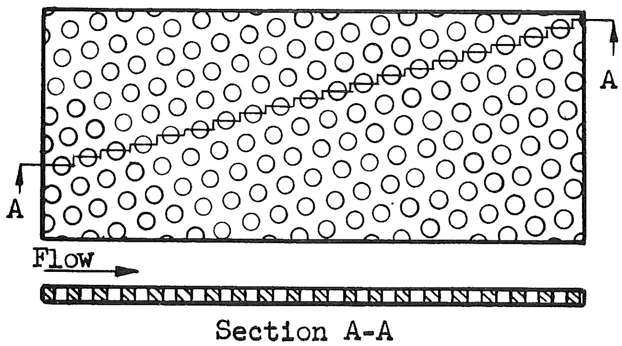

22.5%-OPEN, PERFORATED WALL
Hole Dia. = 1/4 In.
Plate Thickness = 1/16 In.

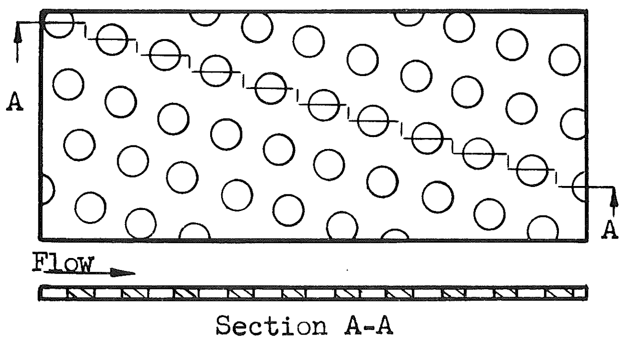

22.5%-OPEN, PERFORATED WALL
Hole Dia. = 1/2 In.
Plate Thickness = 1/16 In.

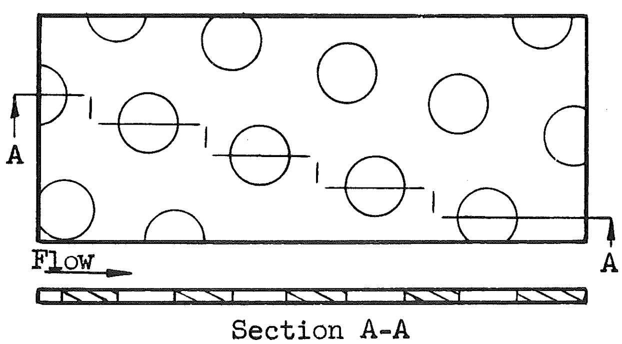

22.5%-OPEN, PERFORATED WALL
Hole Dia. = 1 In.
Plate Thickness = 1/16 In.

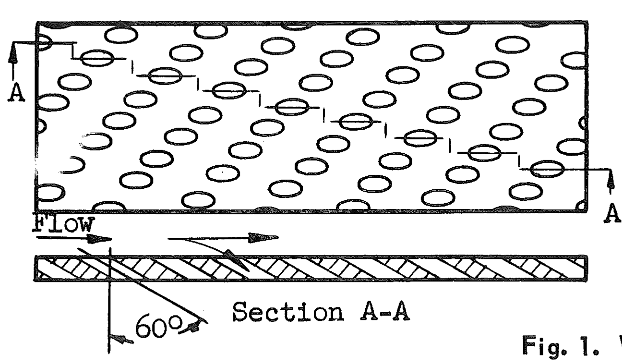

6%-OPEN, INCLINED-HOLE WALL
Hole Dia. = 1/4 In.
Plate Thickness = 1/4 In.

Fig. 1. Walls Tested

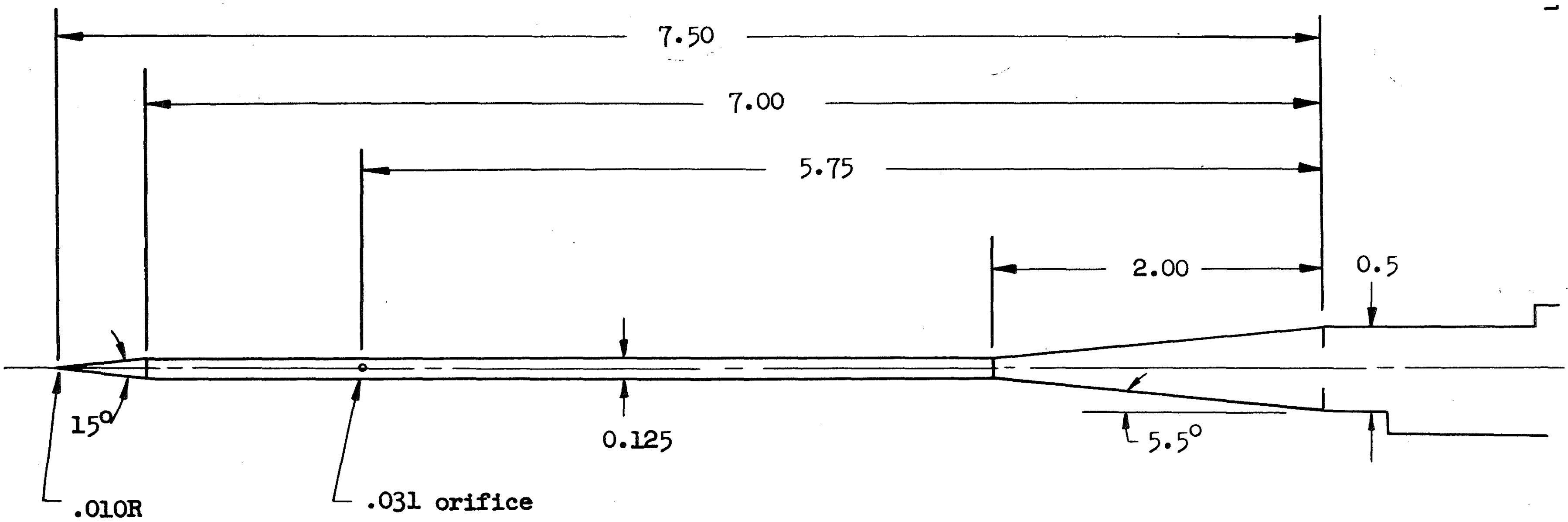

NOTE: All dimensions in inches

Fig. 2. Pressure Survey Probe

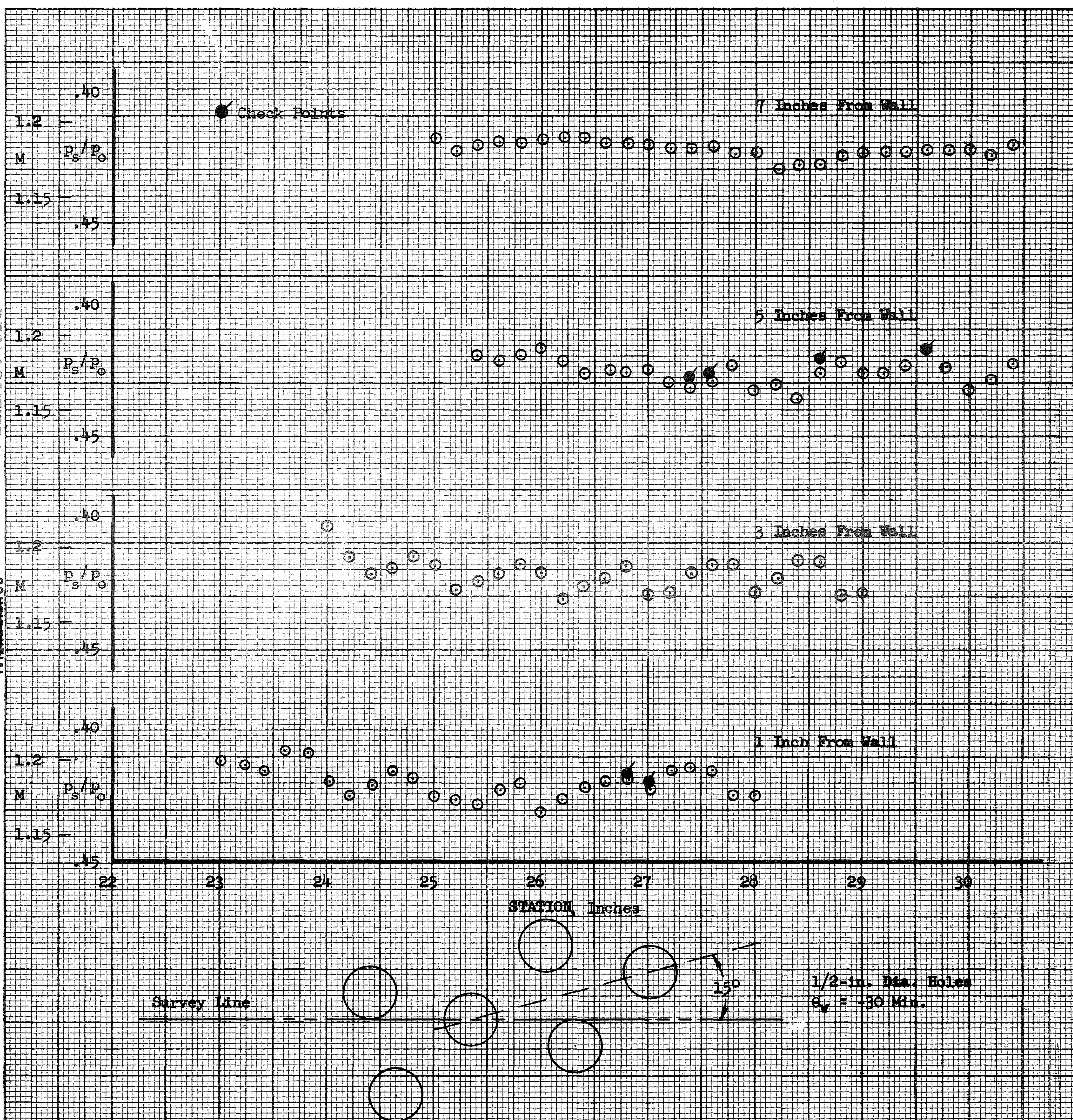

TM 020
005A, 016A, 029A, 038

Fig. 3. Pressure Distributions for ½-in. Diameter Holes, at $M = 1.20$

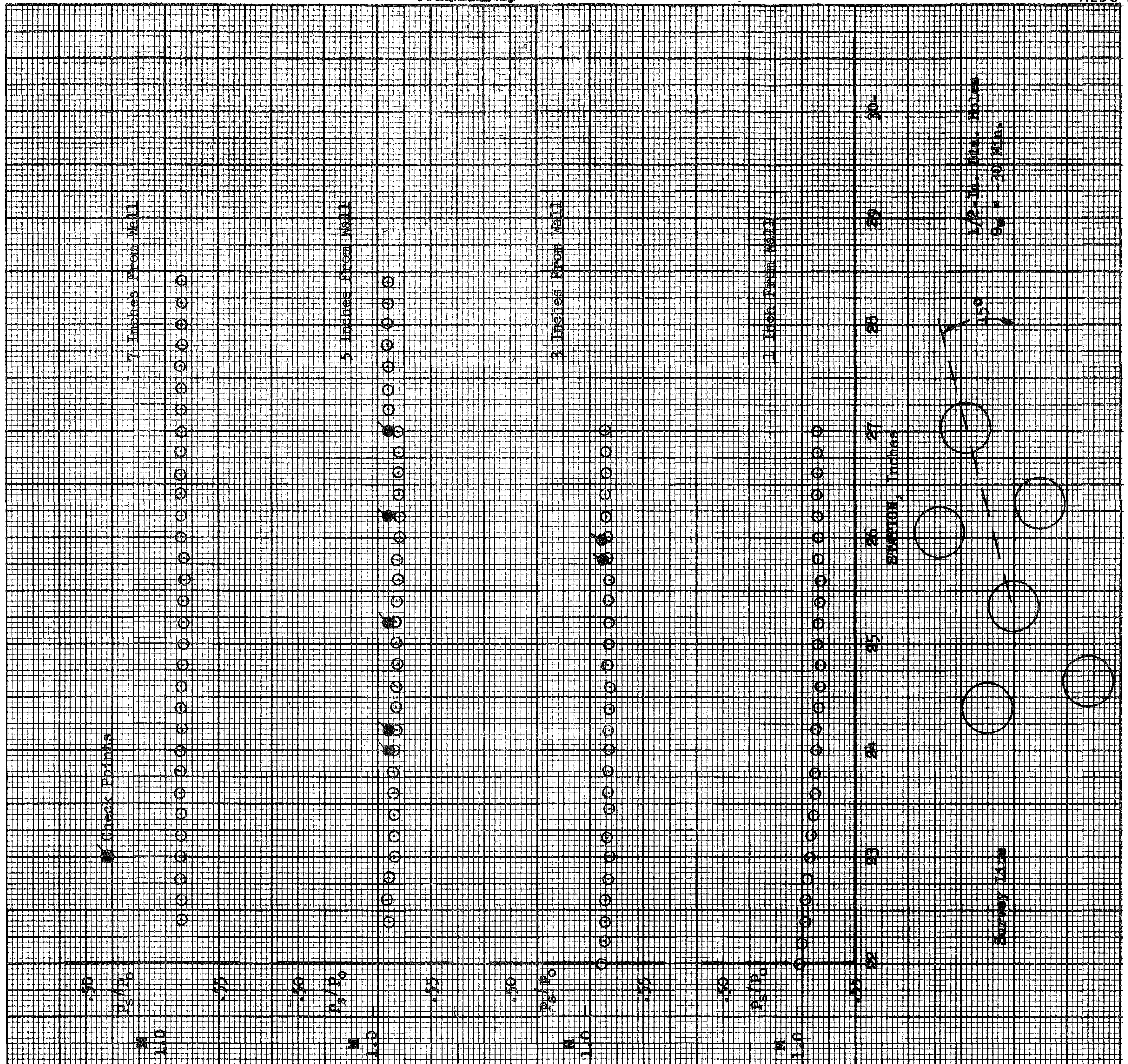

TM 020
005A, 016A, 029A, 038

Fig. 4. Pressure Distributions for ½-in. Diameter Holes, at $M = 1.00$

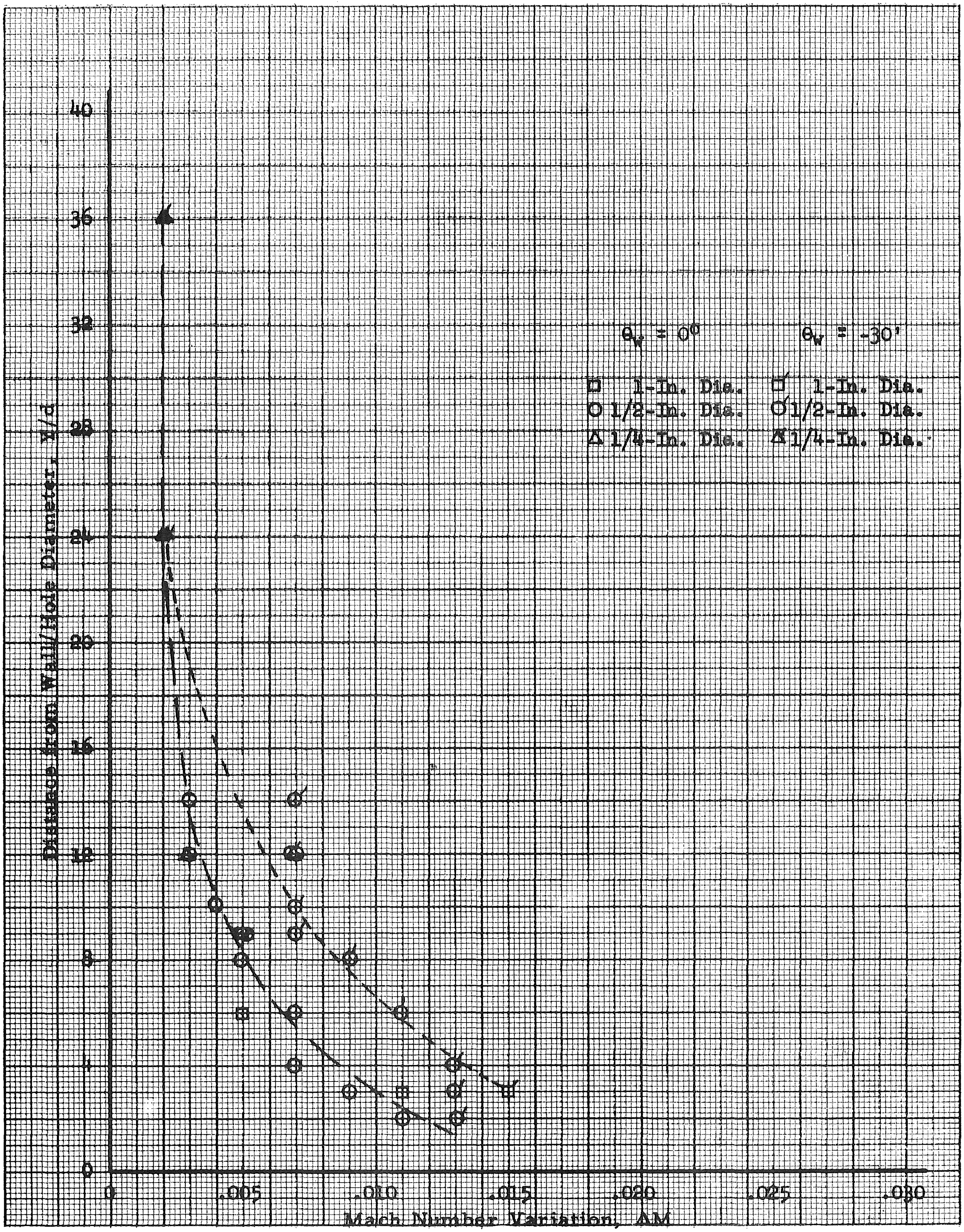

Fig. 5. Decay Profile for Conventional Perforations, at $M = 1.20$

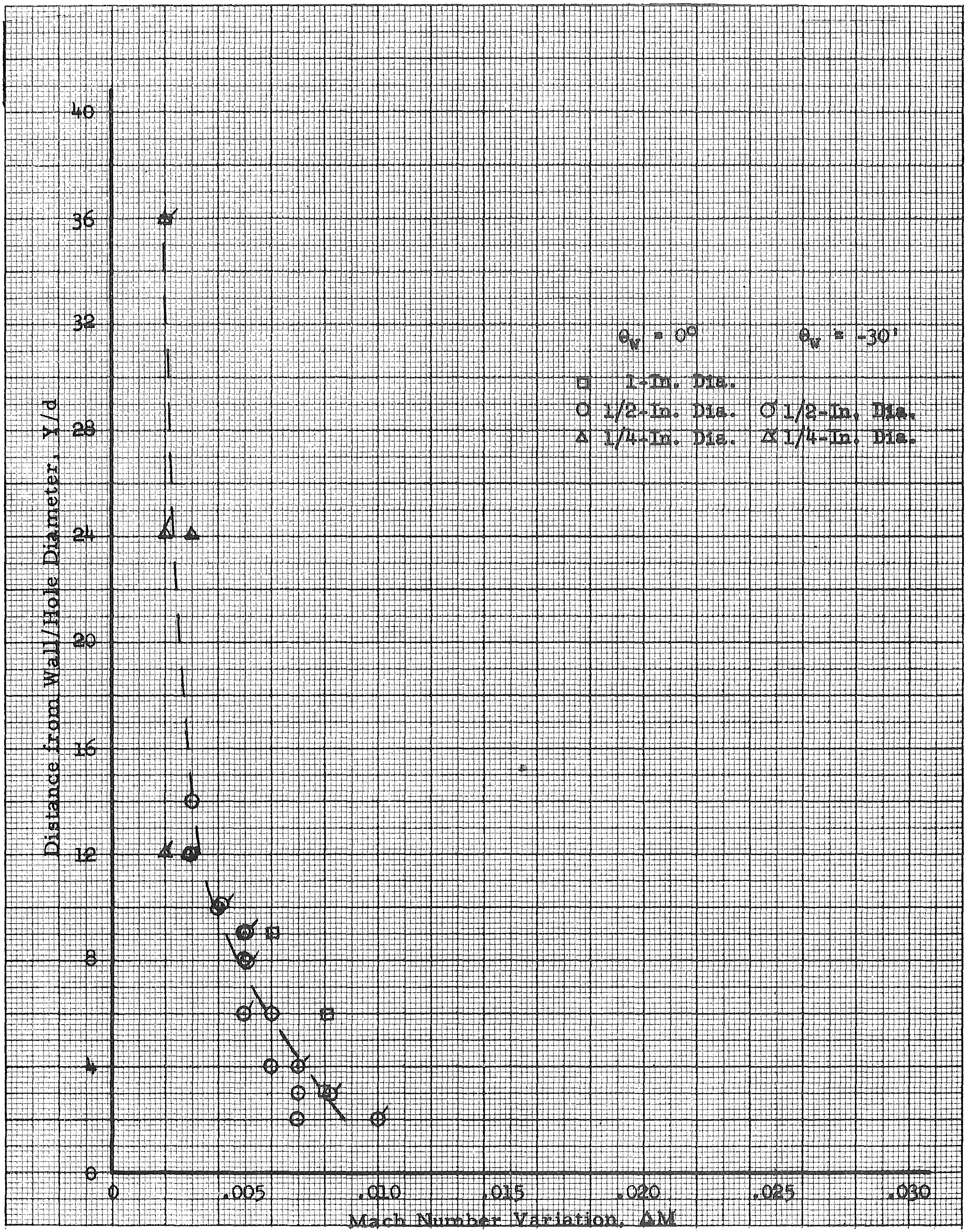

Fig. 6. Decay Profile for Conventional Perforations, at $M = 1.10$

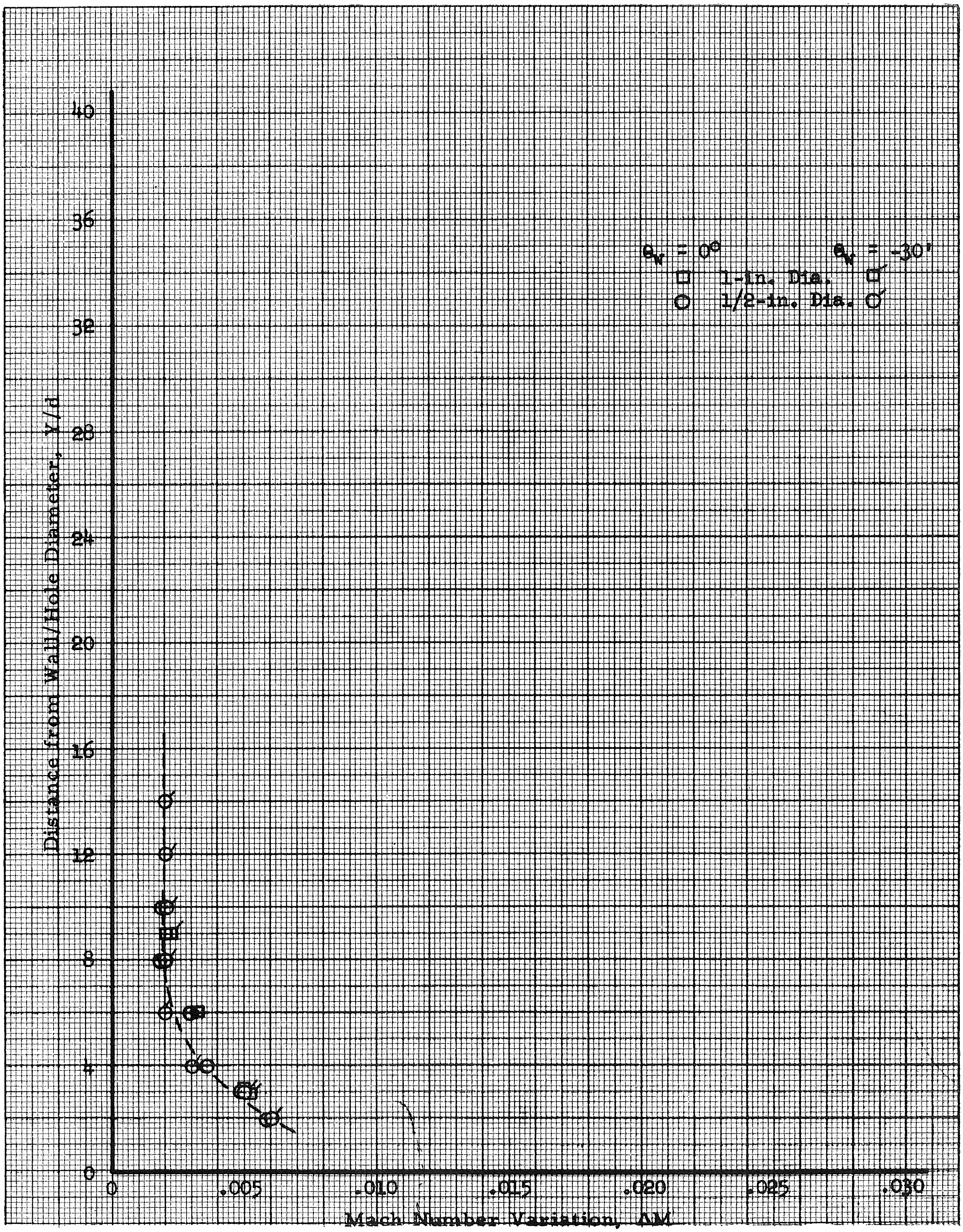

Fig. 7. Decay Profile for Conventional Perforations, at $M = 1.00$

[redacted]

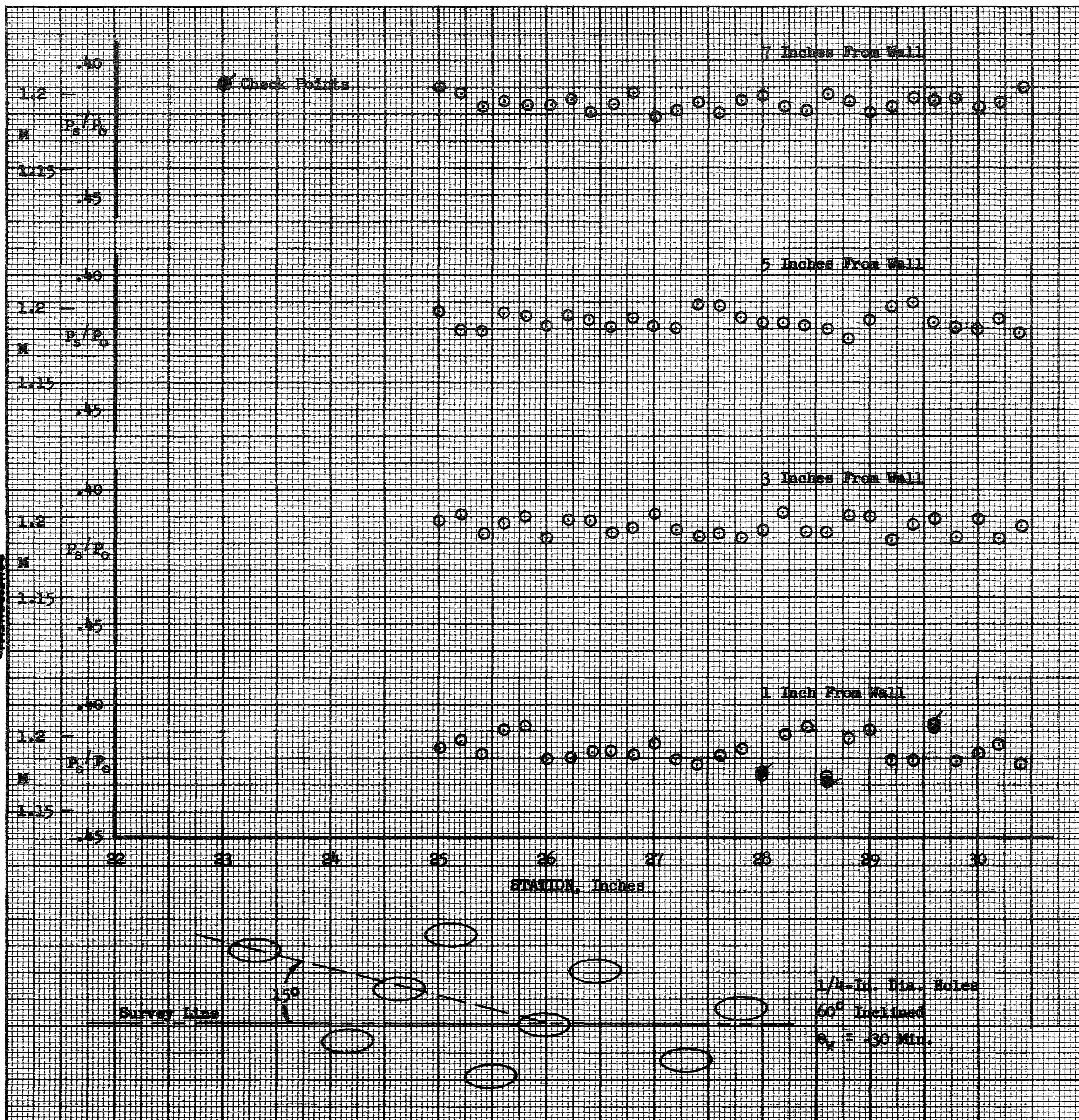

Fig. 8. Pressure Distributions for ¼-in. Holes, Axes Inclined 60°, at M = 1.20

TM020
046, 050, 051, 054

[redacted]

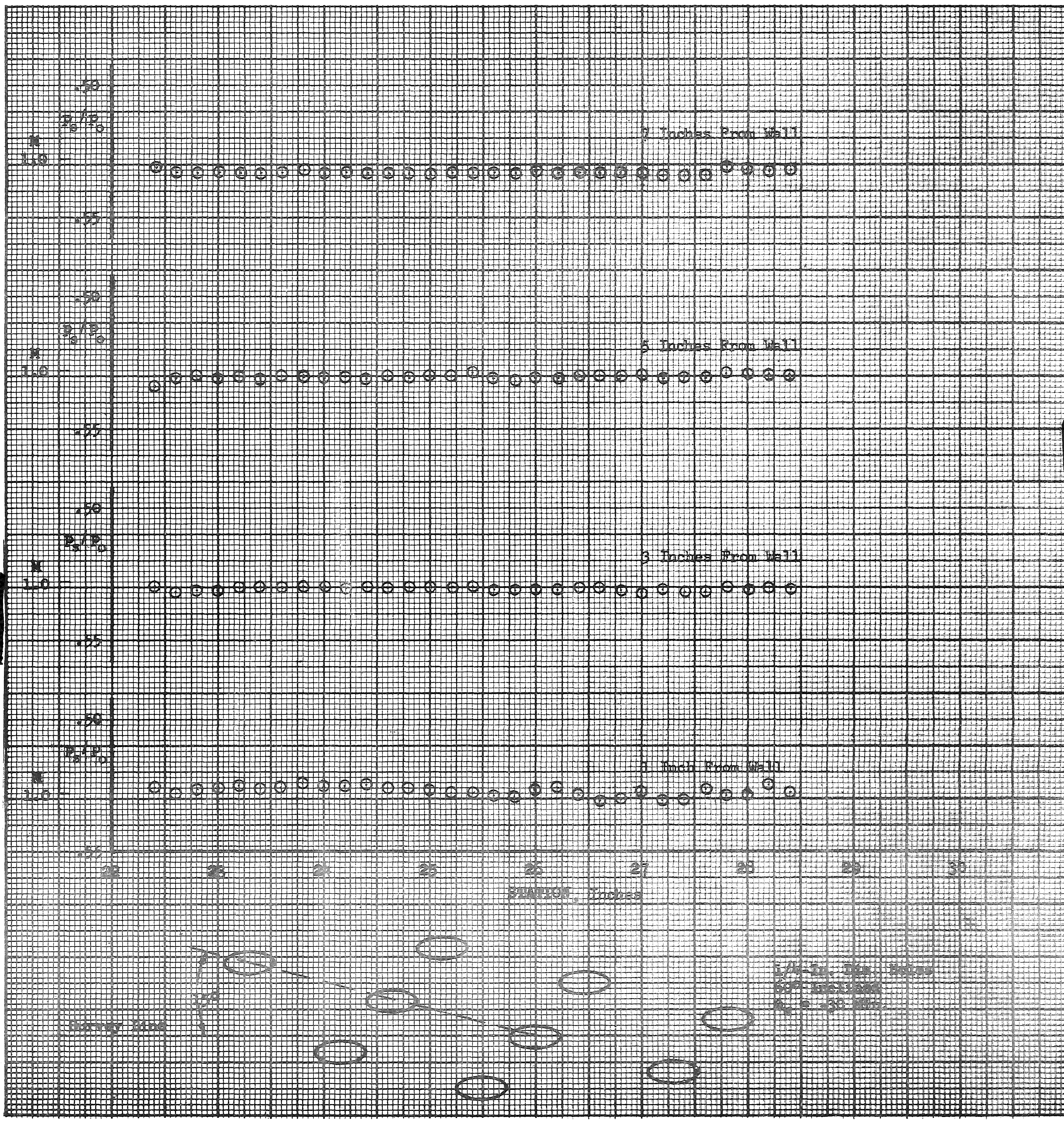

TM 020
046, 050, 051, 054

Fig. 9. Pressure Distributions for ¼-in. Holes, Axes Inclined 60°, at $M = 1.00$

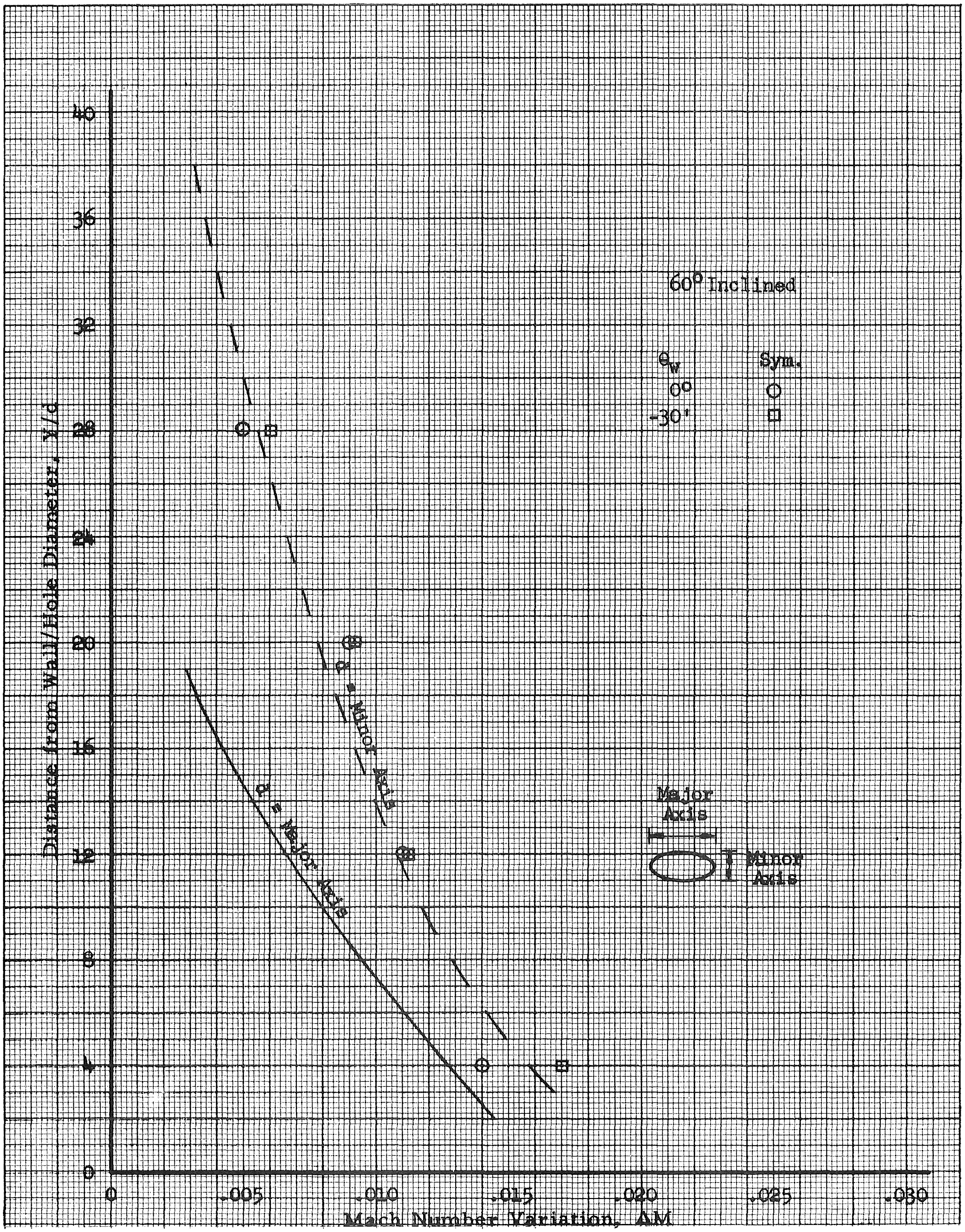

Fig. 10. Decay Profile for Holes with Axes Inclined 60°, at $M = 1.20$

[redacted]

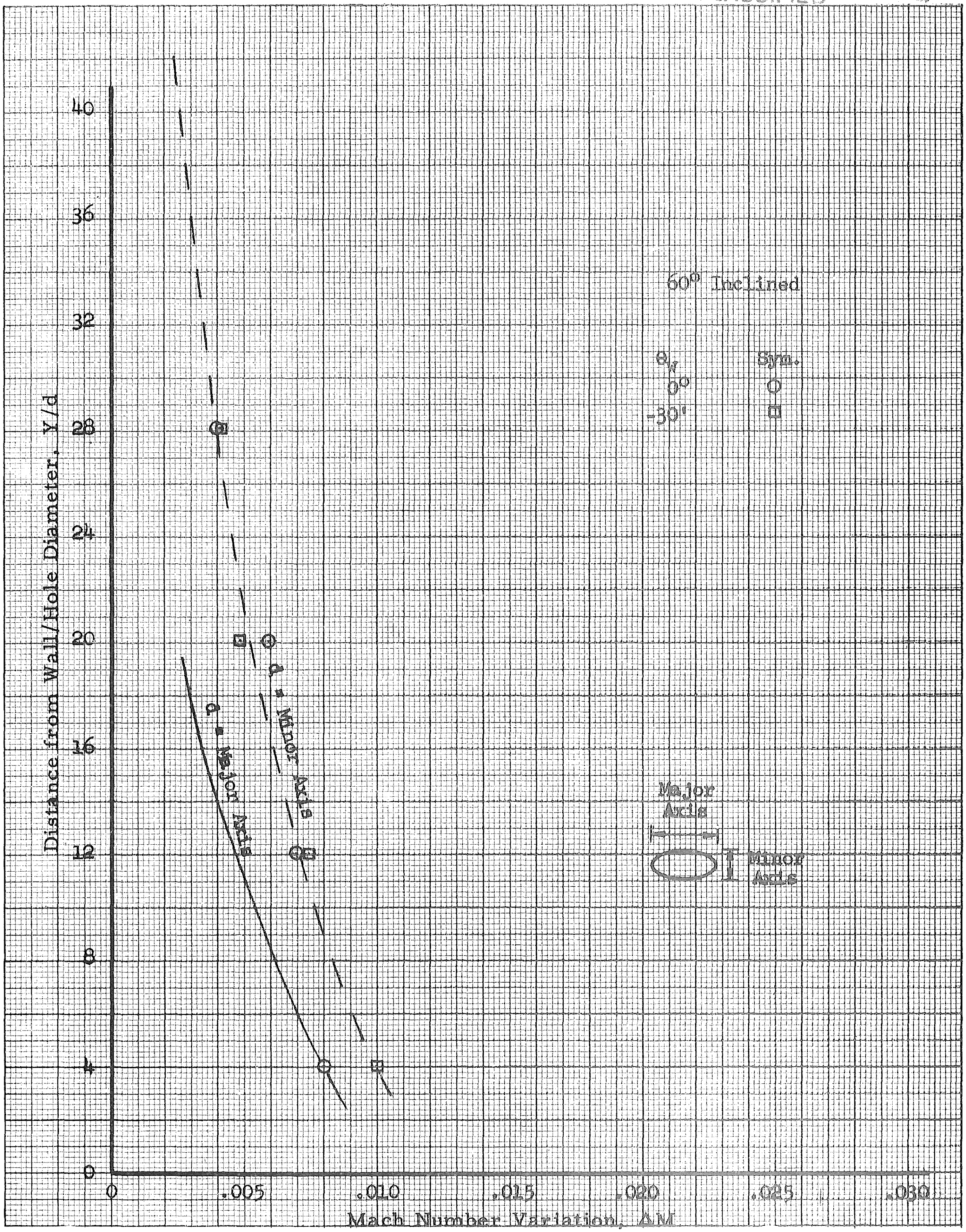

Fig. 11. Decay Profile for Holes with Axes Inclined 60°, at $M = 1.10$

[redacted]

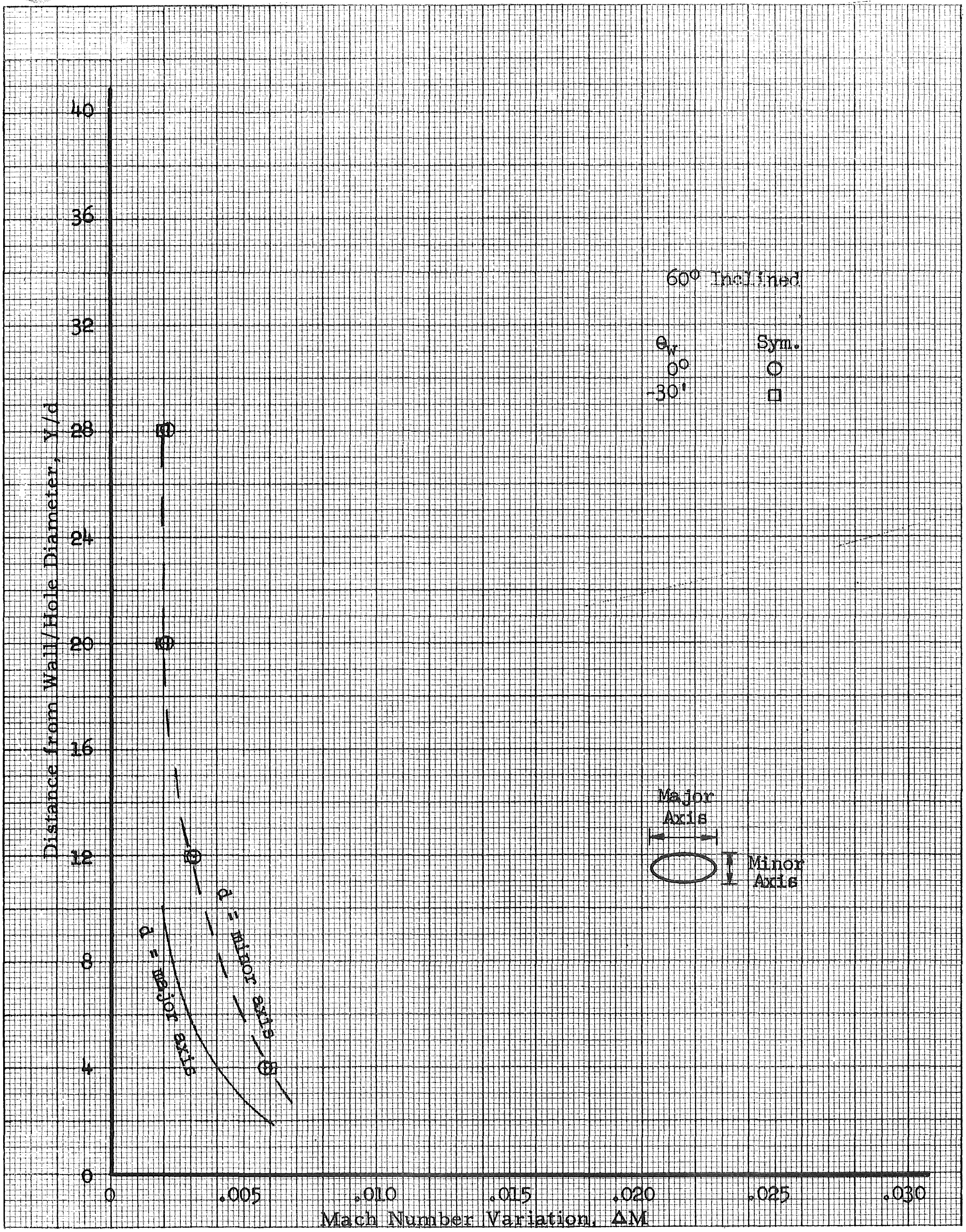

Fig. 12. Decay Profile for Holes with Axes Inclined 60°, at M = 1.00